ARTICLE

Cell research (2004); 14 (2): 161-168
http://www.cell-research.com

Influence of expressed TRAIL on biophysical properties of the human leukemic cell line Jurkat

Kai CHEN[1,*], Dan LI[1,*], Yu Hui JIANG[1], Wei Juan YAO[1], Xin Juan WANG[2], Xiao Chao WEI[2], Jing GAO[3], Li De XIE[1], Zong Yi YAN[4], Zong Yao WEN[1**], Shu CHIEN[5]

[1]*Hemorheology Center, Department of Biophysics, School of Basic Medical Sciences, Peking University, Beijing, 100083, China.*
[2]*Department of Biochemical and Molecular Biology, School of Basic Medical Sciences, Peking University, Beijing, 100083, China.*
[3]*Department of Urology, Medical Center, New York University, USA.*
[4]*Department of Mechanics and Engineering Science, Peking University, Beijing 100871, China.*
[5]*Department of Bioengineering and Whitaker Institute of Biomedical Engineering, University of California, San Diego, La Jolla, CA 92093-0412, USA*

ABSTRACT

The cDNA fragment of human *TRAIL* (TNF-related apoptosis inducing ligand) was cloned into RevTet-On, a Tet-regulated and high-level gene expression system. The gene expression system was constructed in a human leukemic cell line: Jurkat. By using RevTet-On TRAIL gene expression system in Jurkat as a cell model, we studied the influence of TRAIL gene on the changes of cellular apoptosis before and after the TRAIL gene expression, which was induced by adding tetracycline derivative doxycycline (Dox). The results indicated that the cellular apoptosis ratio was largely dependent on the TRAIL gene expression level. Moreover, it was found that the apoptosis-inducing TRAIL could cause significant changes in the biophysical properties of Jurkat cells. The cell surface charge density decreased, the membrane fluidity declined, the elastic coefficients K_1 increased, and the proportion of α-helix in membrane protein secondary structure decreased. Thus, the apoptosis-inducing TRAIL gene caused significant changes on the biomechanic properties of Jurkat cells.

Keywords: TRAIL, Tet gene expression system, Jurkat, apoptosis.

INTRODUCTION

Two major apoptosis pathways have been defined in mammalian cells, the Fas/TNF-R1 death receptor pathway and the mitochondria pathway[1, 2]. TRAIL (TNF-Related Apoptosis Inducing Ligand), also called Apop2 Ligand, belongs to the TNF super-family. In 1995, TRAIL was identified and characterized as a member of the TNF family of death-inducing ligand[3]. As a characteristic type II transmembrane protein, TRAIL shows the highest homology with Fas-L, sharing 28% amino acid identity in the extracellular receptor-binding motif. Unlike most other members of the TNF ligand family, TRAIL has a very short cytoplasmic domain, comprising only 17 amino acids. In addition, no conservation exists within the cytoplasmic region between the human and murine sequences, suggesting that this domain is unlikely to be involved in transmitting cellular signals[3].

TRAIL is widely distributed in normal tissues and cells [3]. A recent study reported that TRAIL is present on the cell surface of mouse T and B cells. $CD3^+$ T cells were found to express TRAIL upon activation with the mitogen phorbol myristate acetate plus ionomycin or via the T cell receptor (anti-CD3) in an activation-dependent manner[4]. Similarly, activation of human T cells with PMA plus ionomycin, anti-CD3, or super antigen was able to induce the expression of TRAIL[3]. Initially it was reported that T cell-enriched cultures of peripheral blood lymphocytes stimulated with interleukin-2 were sensitive to TRAIL-mediated killing[5]. However, these findings have not been reproduced[3]. So far, the only reproducible effects of TRAIL in mediating apoptosis have been reported in transformed cell line[3-5] and hematological malignancies[4, 7]. Other researches of TRAIL were mainly focused on its signaling pathways and its selectivity to induce tumor cell apoptosis[8-11]. To the best of our knowledge, there have been no reports as to how it affects the biophysical properties

*These authors contributed equally to this work.
**Correspondence: Zong Yao WEN,
Tel: 0086-10-62092419; E-mail: rheol@mail.bjmu.edu.cn

of tumor cells.

As it is well known, RevTet-On gene expression system[12] containing Dox possesses excellences such as : the strict open/close function, the strong singularity, the high inducement ratio and expression level and the low toxicity. So the system provides a powerful tool to study eukaryotic gene expression. In the present study, we constructed a Tet-On controlled gene expression system of TRAIL in the human leukemic cell line Jurkat, which was used as a cell model to study the changes in biophysical properties of the Jurkat cells.

MATERIALS AND METHODS

Construction of retroviral plasmids

The RevTet-On system, which includes pRevTet-On and pRev-TRE vectors and the RetroPack PT67 cell line, was purchased from CLONTECH, Palo Alto, California, USA. TRAIL gene was obtained from a human placenta cDNA library (CLONTECH) by PCR. The PCR primers were: 5'-AAGCTTATGGCTATGATGGAGGT-CCAGGGGGGAC-3' and 5'-AAGCTTTTAGCCAACTAAAAA-GGCCCCGAAAAAACTGGC-3'. The PCR product was cloned into an intermediate vector PCR-2 (Invitrogen, Carlsbad, California, USA) and then linked into pLNCX to form vector pLNCX-TRAIL. The Tet-regulated vector pRev-TRE-TRAIL was constructed in the same manner.

Cell culture

The retroviral packaging cell line PT67 and the human leukemic cell line Jurkat were maintained in Dulbecco's modified essential medium and RPMI 1640 containing 10% fetal bovine serum.

Transfections of packaging cells PT67

The packaging cells PT67 were cultured in a 60-mm plate at a density of 50-80%, 24 h before transfection. The cells were washed with DMEM twice and incubated with 2 ml DMEM before transfection with 10 μg of plasmid DNA by Lipofectin method (Life Technology, GIBCO BRL). To obtain stable virus-producing cell lines, the packaging cells transfected with retroviral plasmids were placed in selection medium 48 h later. The regulatory vector Tet-On carrying the neomycin gene served as a selectable marker. For G418 selection, cells were cultured in presence of G418 (0.4 mg/ml, GIBCO) for two weeks. The cells carrying pRev-TRE and pRev-TRE-TRAIL were selected in the presence of hygromycin B (0.06 mg/ml, SIGMA) for two weeks.

Establishment of RevTet-On TRAIL gene expression system in Jurkat cell line[11]

Jurkat cells were kept for 24 h before infection. The medium from packaging cells containing virus were collected, filtered through a 0.45 μm filter, and added to the Jurkat cells in the presence of Polybrene (4 μg/μl, SIGMA). The medium was replaced 4 h later. 3-6 serial infections were performed to increase the efficiency of infection. 48 h after infection, the cells were subjected to G418 or hygromycin selection. The Jurkat cells, which were serially infected with virus-containing media, pRev-Tet-On virus and pRevTRE-TRAIL. Hence they possessed stable resistance to G418 and hygromycin, and were called Jurkat-RevTet-On-TRE-TRAIL(Jurkat3T).

Induction of gene expression and measurement of apoptosis by the bi-parameter method

Cells mentioned above were added to a medium containing Dox (0, 0.01, 0.1, 1, 5, 10 μg/ml, SIGMA). After 48 h, TRAIL protein expression was detected by Western blot. The apoptosis ratio of cells was measured by Flow cytometry.

Confocal microscopy (CLSM) analysis

2×10^6 cells were washed twice with PBS (phosphate-buffered saline, pH 7.4). The sample was fixed in 3.7% formaldehyde for 10 min at room temperature. After washing twice in PBS, the cells were resuspended in 0.1% Triton X-100/PBS for 5 min at room temperature. Then, the cells were incubated in 1% BSA/PBS for 30 min to reduce the nonspecific binding and observed with a confocal laser scanning microscope (Leica Lasertechnik, Germany). A 580 nm long pass filter was used in the fluorescence detection path. The images were collected using a 100×oil immersion objective. Series of 2× optically zoomed confocal sections, 1-2 mm apart, were scanned, with each image averaged by 16 line scans.

Measurement of cell electrophoretic mobility

Jurkat and Jurkat-RevTet-On-TRE-TRAIL induced with Dox (0-10 μg/ml) for 48 h were collected by centrifugation (1000 rpm, 5min). The cell concentration was adjusted to 2×10^6 cells/ml. The cell electrophoretic mobility was measured with a LIANG-100 electrophoresis meter (Shanghai Medical University, Shanghai, China). 100 cells were randomly selected for measurement.

Measurement of membrane fluidity

Jurkat and Jurkat-RevTet-On-TRE-TRAIL induced with Dox (0-10 μg/ml) for 48 h were collected by centrifugation (1000 rpm, 5 min). After washing twice with PBS, the cell concentration was adjusted to 2×10^6 cells/ml. Each cell solution was mixed with the same volume of DPH solution (2×10^{-6}M). After 30 min incubation (37 °C) and centrifugation (1000 rpm, 5 min), the supernatant was removed and the cells were resuspended in PBS. The fluorescence polarization angle P of each tube was measured with a Fluorescence Spectrophotometer within 2 h and calculated according to following equation:

$P=(I_{VV} - GI_{VH})/(I_{VV} + GI_{VH})$

where I_{VV} was the fluorescence identity when polarizer and polarization checker were both at a vertical angle. I_{VH} was the fluorenscence identity when the polarizer was at a vertical angle and the polarization checker was at a horizontal angle. G was the correction factor. According to Azumi[13], $G=I_{HV}/I_{HH}$, where I_{HH} was the fluorescence identity when the polarizer and polarization checker were both at horizontal angles. I_{HV} was the fluoresence identity when the polarizer was at a horizontal angle and the polarizaition checker was at a vertical angle. The microviscosity η, which represents the membrane fluidity, was then calculated from the value of P[13]:

$\eta=2P/(0.46-P)$.

Measurement of the change of secondary structure in cell protein

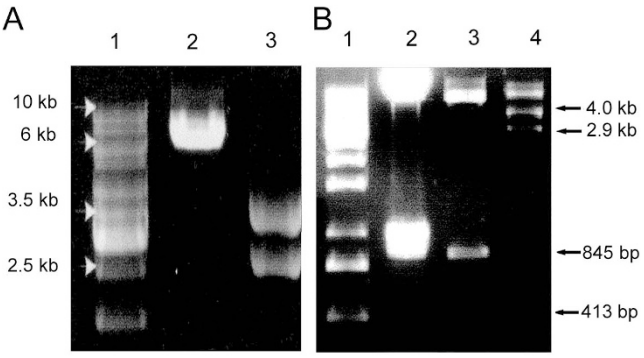

Fig 1. Plasmids construction.
(**A**) 1. Marker;
2. pRev-Tet-On with *Bam* HI;
3. pRev-TRE-TRAIL with Ssp I+ *Hind* III.
(**B**) 1.Marker
2. pLNCX-TRAIL with *Hind* III.
3. pRev-TRE-TRAIL with *Hind* III;
4. pRev-TRE-TRAIL with *Ssp* I.

Jurkat and Jurkat-RevTet-On-TRE-TRAIL induced with Dox (0-10 μg/ml, SIGMA) for 48 h were collected by centrifugation (1000 rpm, 5 min). Then distilled H_2O was added to each tube. 30 min later, the supernatant of each tube was removed by centrifugation (10,000 rpm, 5 min). 100 μl of heavy water was added to each tube. 30 μl solution of each tube was taken out for measurement to obtain the proportion of secondary structure in different cell proteins by using an FT-IR Spectrometer (Bio-RAD Company). The scan solution was $4cm^{-1}$ and the scan range was $1500\text{-}1800cm^{-1}$.

Measurement of cell viscoelastic properties[13]

Jurkat and Jurkat-RevTet-On-TRE-TRAIL induced with Dox (0-10 μg/ml) for 48 hours were collected by centrifugation (1000 rpm, 5 min). Cell viscoelastic properties were measured with micropipette aspiration system, which was composed of an inverted microscope, a micromanipulator, a video recorder, a pressure control and recorder system, and a pipette. 0.5 ml of the cell suspension (1×10^6 cells/ml) was placed in a chamber located on the specimen stage of the microscope. The internal diameters of the micropipette were 2.4-3.1 μm. The time course of cell deformation was continuously recorded on the video recorder. The sequential photographs were taken from the recorded video image during single-frame replay on the video monitor every 120 ms. The length of the cell tongue aspirated into the micropipette was determined as a function of time. The time history of deformation typically showed an initial rapid phase followed by a slow creep, similar to the behavior of peripheral blood leukocytes studied previously[13]. A standard solid viscoelastic model was used to fit the experimental data. The equation of this model was as follows:

$$\sigma+(\mu/K_2)\partial\sigma/\partial t = K_1\varepsilon+\mu[1+(K_1/K_2)]\partial\varepsilon/\partial t$$

Where σ and ε are the stress and the strain, and $\partial\sigma/\partial t$ and $\partial\varepsilon/\partial t$ are partial derivatives of the stress and the strain as functions of time, respectively. K_1 and K_2 are elastic elements, and μ is a viscous element.

Each sample was scanned 200 times. Student *t*-test and ANOVA were used for the statistical analysis of experiment data with the statistic analysis software SPSS.

RESULTS

Establishment of RevTet-On TRAIL gene expression system and induction of *TRAIL* in Jurkat cell line

From recombinant pRevTet-On after purification, the 7.6 kb fragment was obtained using *Bam* HI, and from recombinant Plasmids pRev-TRE, the 3.6 kb and 2.8 kb fragments were obtained using *Ssp*I and *Hind* III. This was consistent with the restriction enzyme map of Plasmids in Fig 1A.

From recombinant plasmid, 6.5 kb and 845 bp were obtained after *Hind* III enzyme cutting. It showed that the objective gene *TRAIL* has been cloned into the recombinant Plasmid. Moreover, in order to identify the orientation, from recombinant Plasmid, the 4.0 kb, 2.9 kb and 413 bp fragments were obtained after *Ssp*I enzyme cutting, as shown in Fig 1B, which showed that the result was consistent with the restriction enzyme map of the plasmids. This fact indicated that the objective gene *TRAIL* has been correctly linked to vector pRev-TRE and it was called pRev-TRE-TRAIL.

By plasmids transfection and antibiotics selection, we constructed a Tet controlled gene expression system of *TRAIL* in Jurkat. Fig 2 shows the growth curves of Jurkat, Jurkat2T and Jurkat3T. And as shown in this figure, there was no significant difference between the three cell lines.

Fig 3 shows the results of Western blot analysis of TRAIL protein expression. Lane 1 indicates the protein markers. Protein in lane 2 was isolated from Jurkat-RevTet-On–TRE-TRAIL induced with Dox (10 μg/ml) for 48 h and that in lane 3 was isolated from Jurkat -RevTet-On–TRE-TRAIL and kept for 48 h without Dox induction (0 μg/ml). The band in lane 2 indicates that the TRAIL protein (molecular weight about 37 kD) was expressed when

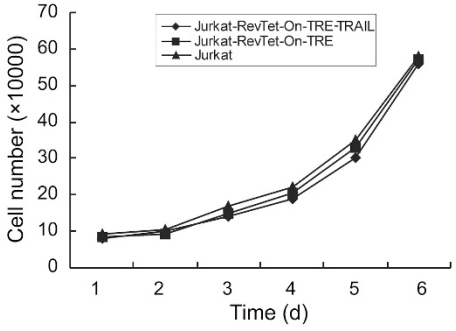

Fig 2. Growth curves of Jurkat, Jurkat 2T and Jurkat 3T.

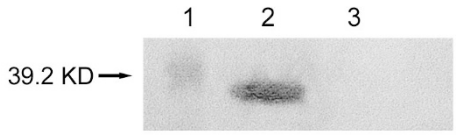

Fig 3. Western blot analysis of TRAIL protein expression. Lane 1: protein markers, Lane 2: protein isolated from Jurkat RevTet-On-TRE-TRAIL induced with Dox (10 μg/ml) for 48 h, Lane 3: protein isolated from Jurkat-RevTet-On-TRE-TRAIL not induced with Dox (0 μg/ml) and kept for 48 h.

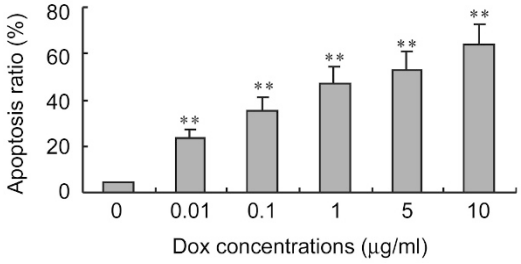

Fig 4. Apoptosis ratio of Jurkat3T induced with different concentrations of Dox measured by flow cytometer. The ratio increased significantly in a dose-dependent manner. Compared with Dox (0 μg/ml) : ** indicates $p<0.01$

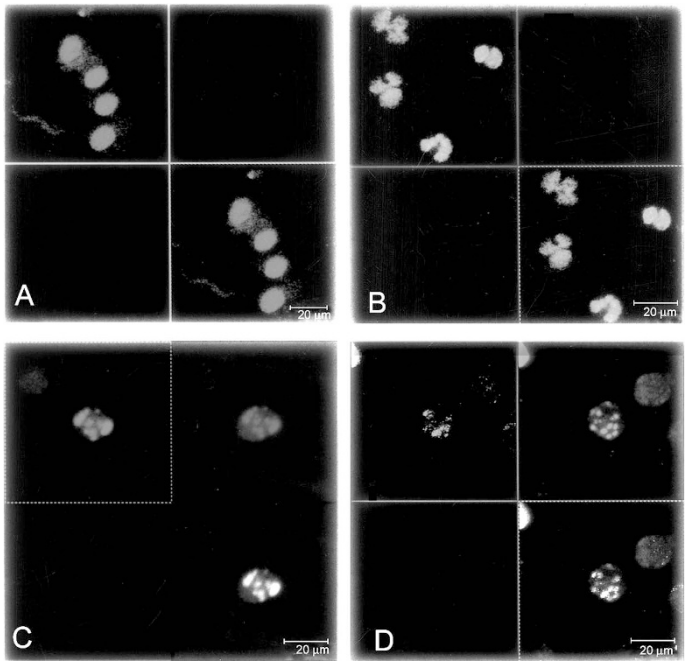

Fig 5. Observation of cell nucleus undergoing apoptosis by confocal laser scanning microscopy. The nucleus of Jurkat3T treated with Dox (0 μg/ml) were regular and integral (A). However, in the cells treated with Dox (0.01 μg/ml), the chromatin were collected under nucleus membrane and the nucleus became into crescent shape or petal (B). In the cells treated with Dox (1 or 10 μg/ml), even appeared apoptotic bodies (C, D).

Jurkat -RevTet-On–TRE-TRAIL was induced with Dox (10 μg/ml) for 48 h. The fact that this band was absent in lane 3 indicated that TRAIL protein was not expressed when Jurkat -RevTet-On–TRE-TRAIL had not been treated with Dox.

As shown in Fig 4, compared with Jurkat3T untreated with Dox (0 μg/ml), the apoptosis ratio of Jurkat3T induced with Dox increased significantly ($p<0.01$) in a dose-dependent manner. The apoptosis ratio had a correlation coefficient of 0.78 with the logarithm of Dox concentration.

Compared with Jurkat3T untreated with Dox (0 μg/ml), Jurkat3T cells expressing TRAIL showed distinct changes. The cells chromatin were collected under nucleus membrane and the nucleus became into crescent shape or petal, and even appeared apoptotic bodies. Furthermore, the apoptosis ratio of Jurkat3T induced with Dox increased significantly in a dose-dependent manner (Fig 5).

As shown in Fig 6, after treating Jurkat with 1 μg /ml concentration of Dox, the Jurkat death ratio increased with time, and the death ratio of Jurkat reached maximum at 60 h.

These facts indicated that the Tet-controlled gene expression system had been constructed successfully and there was no significant influence on cell growth of Jurkat after transgene. However, the apoptosis ratio of Jurkat3T increased significantly with Dox.

Cell electrophoretic mobility

Tab 1 shows the results of measurement of the electrophoretic mobility of different groups of cells. There was no significant difference between Jurkat cells (Group 1) and Jurkat3T cells untreated with Dox (Group 2). Jurkat3T induced with different Dox concentrations (0.01, 0.1, 1, 5, 10 μg/ml in Groups 3-7, respectively) have a dose-dependent decrease in electrophoretic mobility ($P<0.01$). The correlation coefficient with the logarithm of the Dox concentration is -0.86.

Membrane fluidity

Tab 2 shows the results of microviscosity of different groups of cells. There was no significant difference between Jurkat cells (Group 1) and Jurkat3T cells untreated with Dox (Group 2). Jurkat3T induced with different Dox concentrations (0.01, 0.1, 1, 5, 10 μg/ml in Groups 3-7, respectively) have a dose-dependent increase in microviscosity ($p<0.01$); the correlation coefficient with the logarithm of the Dox concentration is 0.91.

The change of secondary structure in cell proteins

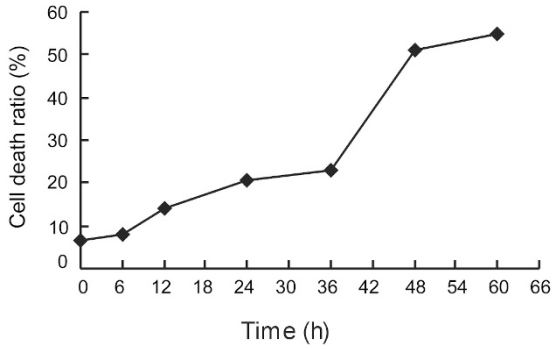

Fig 6. The relation curve between cell death ratio and time after treating Jurkat3T with Dox (1 μg/ml). The death ratio increased with time, and reached maximum at 60 h.

There was no significant difference between Jurkat cells (Group 1) and Jurkat3T cells untreated with Dox (Group 2). While in Jurkat3T cells induced with different Dox concentrations (0.01, 0.1, 1, 5, 10 μg/ml in Groups 3-7, respectively) the proportion of α-helix decreased significantly ($P<0.01$). No apparent orderliness was found in proportions of β-pleated sheets and β bend after the induction with Dox (Tab 3).

Viscoelastic coefficients of different groups of Jurkat cells

The elastic coefficient K_2 and the viscosity coefficient were not significantly changed among all groups. The

Tab 1. The electrophoretic mobility of different groups of cells ($\bar{x} \pm SD$).

	1	2	3	4	5	6	7
Electrophoretic mobility (μm/s/V/cm)	1.926 ± 0.136	1.894 ± 0.280	1.559 ± 0.329*	1.430 ± 0.349*	1.393 ± 0.19*	1.376 ± 0.273*	1.320 ± 0.322*

Compared with Group 2: *: $p < 0.01$

1: Jurkat cells; 2: Jurkat3T cells untreated with Dox (0 μg/ml); 3-7: Jurkat3T cells induced with Dox at 0.01, 0.1, 1, 5, and 10 μg/ml, respectively.

Tab 2. The membrane microviscosity of different groups of cells ($\bar{x} \pm SD$).

	1	2	3	4	5	6	7
Microviscosity (Poise)	0.97	0.95	1.24	1.28	1.31	1.38	1.43
Mean ± S.D.	± 0.07	± 0.08	± 0.06*	± 0.04*	± 0.05*	± 0.05*	± 0.06*

Compared with group 2: *: $p < 0.01$

1: Jurkat cells; 2:Jurkat3T cells untreated with Dox (0 μg/ml); 3-7 : Jurkat3T cells induced with Dox at 0.01, 0.1, 1, 5, and 10 μg/ml, respectively.

elastic coefficient K_1 is not significantly different between Jurkat cells (Group 1) and Jurkat3T cells untreated with Dox (Group 2). Jurkat3T induced with different Dox concentrations (0.01, 0.1, 1, 5, 10 μg/ml in Groups 3-7, respectively), however, have a dose-dependent increase in K_1 ($P<0.01$) (Tab 4).

DISCUSSION

TRAIL is known to have a number of biological actions, including the induction of apoptosis. However, the influence of TRAIL on biophysical properties of cells such as Jurkat is still unknown.

Treatment with Dox caused significant alterations in the membrane microstructure of the Jurkat3T cells. These changes include the decrease in the proportion of α-helix in cell protein, and increase in membrane microviscosity. Thus, the induction of TRAIL by Dox, binding with the ligand-receptors[15, 16] on the membrane of Jurkat, caused these biophysical changes in Jurkat3T in addition to its capability to increase apoptosis. The important role of TRAIL in causing these biophysical changes is further demonstrated by the dose dependency of these changes in relation to the Dox concentration.

The decrease in cell electrophoretic mobility following TRAIL expression indicates a decrease in the negative surface potential on the cell surface, which was caused by acetylneuraminate of glycoprotein[17]. The negative charge of cells mainly came from the carboxyl groups of sialic acids on the cell surface[18]. When TRAIL was expressed, the ensuing ligand-receptor binding may affect the conformation and function of the molecules on membrane. For example, the binding may lead to partial removal of sialic acids from the membrane and thus the surface charge was reduced[18]. This is manifested not only in the electrophoretic mobility, but also in the changes in the secondary structure proportions in membrane proteins. These alterations in the structure and function of the cell may signal the cell to undergoing apoptosis.

When the TRAIL gene is expressed and the TRAIL protein binds to its receptors on the membrane, it would influence the fluidity of membrane lipid to cause a decline of membrane fluidity[15]. The membrane fluidity is inversely related to the microviscosity η. The Jurkat cell membrane microviscosity increased, i.e., the fluidity decreased, with the TRAIL expression level. The membrane fluidity is mainly determined by the membrane lipid composition (cholesterol, the degree of saturation and chain length of the fatty acids, and the proportion of lecithin and sphingomyelin), as well as membrane protein-lipid interactions. One of the plasma membrane alterations in the early stages of apoptosis is the translocation of

Tab 3. The proportion of secondary structure in different types of cell proteins of different groups of cells

	1	2	3	4	5	6	7
α-helix	0.4452 ± 0.0356	0.4462 ± 0.0356	0.3852 ± 0.0308*	0.3795 ± 0.0303*	0.3738 ± 0.0299*	0.3687 ± 0.0295*	0.3641 ± 0.0291*
β-pleated sheets	0.3227 ± 0.0258	0.3222 ± 0.0257	0.2817 ± 0.0225	0.4027 ± 0.0322	0.2221 ± 0.0177	0.4355 ± 0.0348	0.4227 ± 0.0338
β-bend	0.2319 ± 0.0185	0.2315 ± 0.0185	0.3330 ± 0.0266	0.2177 ± 0.0174	0.4040 ± 0.0323	0.1957 ± 0.0156	0.2130 ± 0.0170

Compared with group 2: *: $p < 0.05$

1: Jurkat cells; 2: Jurkat3T cells untreated with Dox (0 μg/ml); 3-7: Jurkat3T cells induced with Dox at 0.01, 0.1, 1, 5, and 10 μg/ml, respectively.

Tab 4. Viscoelastic coefficients of different groups of cells ($\bar{x}$±SD).

	1	2	3	4	5	6	7
K_1(N/m$^{2)}$	83.2 ± 34.1	84.1 ± 35.3*	94.1 ± 36.2**	103.1 ± 46.8**	125.1 ± 48.4**	154.2 ± 59.4**	186.3 ± 61.2**
K_2(N/m^2)	21.4 ± 11.1	21.7 ± 11.3*	22.1 ± 11.6*	22.2 ± 12.3*	23.2 ± 12.1*	23.9 ± 13.4*	24.1 ± 14.1*
μ(N.s/m^2)	4.1 ± 2.7	4.3 ± 2.8*	4.5 ± 2.0*	4.7 ± 1.3*	4.6 ± 2.2*	4.5 ± 2.0*	4.4 ± 2.9*

Compared with group 2: *: $P < 0.05$, **: $P < 0.01$

1: Jurkat cells; 2: Jurkat3T cells untreated with Dox (0 μg/ml); 3-7: Jurkat3T cells induced with Dox at 0.01, 0.1, 1, 5, and 10 μg/ml, respectively.

phosphatidylserine (PS) from the inner side of the plasma membrane to the outer layer, by which PS becomes exposed at the external surface of the cell[20, 21]. Moreover, some biological molecules, such as molecules in cytoskeleton protein were disintegrated during the apoptosis. These changes can also influence the fluidity of the membrane lipid in Jurkat[22].

α-helix structures in cell protein play a significant role in transducing the extracellular signals into the cell, and the secondary structure in proteins of the cell may change during this process. The decrease in α-helix proportion following TRAIL expression may reflect the effect of its binding to the related receptor on the cell. When the apoptosis signal transmitted into Jurkat after TRAIL expression, it would lead to the changes of α-helix structure which may turn into β-pleated sheets or β-bend in the cell proteins and accelerate the apoptosis of cancer cells.

The increase in the elastic coefficient K_1 after TRAIL expression indicates that the cells' maximum deformation became smaller, i.e., the cells became more rigid.

The membrane biomechanics is closely related to the microstructure. The membrane elastic coefficient of Jurkat increased with the TRAIL expression level. The membrane elastic coefficient is mainly determined by the composition of cytoskeleton protein and the membrane lipid, as well as the interactions between the molecules of protein and lipid in the membrane. When the TRAIL gene was expressed and binded to its receptors on the membrane, it would change the structure of membrane molecules to cause a decline of membrane biomechanics properties[17, 23].

On all accounts, from above experiments results, we can see that the changes of biophysical properties (including the increase of the membrane microviscosity η, the membrane elastic coefficient K_1 as well as the decrease in cell electrophoretic mobility) of Jurkat may come from the variations of acetylneuraminate composition in the glycoprotein and the protein's proportions after the TRAIL expression, but it should be manifested by further experiments.

Our new findings can be summarized as follows. First, we constructed the RevTet-On TRAIL gene expression system on human leukemic cell line Jurkat. The TRAIL protein was expressed in the presence of the tetracycline derivative doxycycline, and, importantly, this expression was able to induce apoptosis. Second, we have elucidated the changes of the membrane microstructure of the Jurkat cell following the TRAIL expression. These changes may be related to the apoptosis induced by TRAIL and also the inhibiting effect of the TRAIL on tumor cells. The present study has laid the foundation for the potential application of TRAIL in the gene therapy of cancers. Third, we combined the biophysical with molecular biology to study the influence of the TRAIL gene on the microstructure of the tumor cells as well as the changes of the biophysics properties of tumor cells before and after apoptosis by regulation of gene expression. We have investigated the biophysical effects of p53 and TFAR19 (TF-1 cells apoptosis-related gene 19) gene on murine erythroleukemia cell line (MEL) [24, 25], and the current work will provide further evidence for the relationship between the biophysics and the tumor gene therapy.

ACKNOWLEDGEMENTS

This work was supported by The National Natural Science Foundation of China (No.30270355, No.39930110) and a Doctoral Funding (No. 20010001082).

Received, Feb 28, 2003
Revised, Mar 28, 2004
Accepted, Mar 29, 2004

REFERENCES

1 Yin XM. Signal transduction mediated by Bid, a pro-death Bcl-2 family proteins, connects the death receptor and mitochondria apoptosis pathways. Cell Res 2000; **10**:161-7.
2 Jiang ZF, Shan Z, Ying LS, Zhong HZ. Induction of apoptosis in purified animal and plant nuclei by *Xenopus* egg extracts. Cell Res 1999; **9**:79-90.
3 Wiley SR, Schooley K, Din PJ, Smolak, et al. Identification and characterization of a new member of the TNF family that induces apoptosis. Immunity 1995; **8**:3672-82.
4 Mariani SM, Krammer PH. Surface expression of TRAIL/Apop2 ligand in activated mouse T and B cells. Eur J Immunol 1998; **28**: 1492-8.
5 Marsters SA, Pitti RM. Activation of apoptosis by apoptosis by Apo-2 ligand is independent of FADD but blocked by CrmA. Current opinion in Biology 1996; **6**:750-2.
6 Pitti RM, Marsters SA, et al. An induction of apoptosis by Apo-2 ligand, a new member of the tumor necrosis factor cytokine family. J Biol Chem 1996; **27**:12687-90.
7 Katisikis P, Garcia ME, et al. ICE-like protease involvement in Fas-induced and activation-induced peripheral blood T cell death apoptosis in HIV infection. TRAIL can mediate activation-induced T cell death in HIV infection. J Exp Med 1997; **186**:1365-72.
8 Yamada H, Tada-Oikawa S, Uchida A, Kawanishi S. TRAIL causes cleavage of bid by caspase-8 and loss of mitochondrial membrane potential resulting in apoptosis in BJAB cells. Biochem Biophys Res Commun 1999; **265**:130-3.
9 Wajant H, Haas E, Schwenzer R, et al. Inhibition of death receptor-mediated gene induction by acycloheximide-sensitive factor occurs at the level of or upstream of Fas-associated death domain protein (FADD). Biol Chem 2000; **275**:24357-66.
10 Kim MR, Lee JY, Park MT, et al. Ionizing radiation can overcome resistance to TRAIL in TRAIL-resistant cancer cells. FEBS Lett 2001; **505**:179-84.
11 Salvucci O, Carsana M, Bersani I, Tragni G, Anichini A.

Antiapoptotic role of endogenous nitric oxide in human melanoma cells. Cancer Res 2001; **61**:318-26.
12 Lottmann H, Vanselow J, Hessabi B, Walther R. The Tet-On system in transgenic mice: inhibition of the mouse pdx-1 gene activity by antisense RNA expression in pancreatic beta-cells. J Mol Med 2001; **79**:321-8.
13 Lin K. Advance of Biochemistry and Biophysics. 1981; 22-5.
14 Long M, Wu HB, Wang, et al. Experimental investigation on viscoelasticity of hepatocytes. Acta Biophysica Sinica 1996; **12**: 169-73. (in Chinese with English abstract)
15 Tartaglia LA, AYRES TM, et al. A novel domain within the 55KD TNF receptor signals cell death. Cell 1993; **74**:845-53.
16 Nagata S. Apoptosis by death factor. Cell 1997; **88**:355-6.
17 Lin KC, Wu BJ. Medical Biophysics. Beijing Medical University, Chinese Union Medical University Union Press 1996; p128-129, 110-20.
18 Wen ZY, Yao WJ, Xie LD, et al. Influence of neuraminidase on the characteristics of microrheology of red blood cells. Clini Hemorheol Microcirc 2000; **23**:51-7.
19 Bohler T, Linderkamp O. Effects of neuraminidase and trypsin on surface charge and aggregability of red cells. Cin Hemorheol 1993; **13**:775-8.
20 Istvãn V, Clemens H, Helag SN, et al. A novel assay for apoptosis Flow cytometric detection of phosphatidylserine expression on early apoptotic cells using fluorescein labeled Annexin V. J Immunol Methods 1995; **184**:39-51.
21 Valerian E, Kagan, James P. Fabisiak, Amma A. Shvedova, et al. Oxidative signaling pathway for externalization of plasma membrane phosphatidylserine during apoptosis. FEBS Lett 2000; **477**:1-7.
22 Ewa J, Adam S, Slawomir C, et al. Apoptosis-independent alterations in membrane dynamics induced by crucumin. Exp Cell Res 1998; **245**:303-12.
23 Yao WJ, Chen K, Wang XJ, et al. Influence of TRAIL gene on biomechanical properties of the human leukemic cell line Jurkat. J Biomech 2002; **35**:1659-63.
24 Yao WJ, Gu L, Sun DG, Ka WB, Wen ZY, Chien S. Wild type p53 gene causes reorganization of cytoskeleton and, difficult migration of murine erythroleukemia cells. Cell Motil Cytoskeleton 2003; **56**:1-12.
25 Gu L, Yao WJ, Yan ZY, et al. Effect of TFAR19 gene on the growth and biophysical properties of mouse erythroleukemia cell line MEL. Sci in China (series C) 2003; **46**:293-301.